Modal Attenuation in Multilayered Coated Waveguides

RI-CHEE CHOU, MEMBER, IEEE, AND SHUNG-WU LEE, FELLOW, IEEE

Abstract—**Propagation and attenuation constants of low-order normal modes in a circular waveguide lined with lossy coating layers are calculated using a generalized dispersion equation. It is found that the use of multilayered coating can significantly enhance modal attenuations over a broader frequency range compared to that for a single-layer coated structure. For a cylinder with radius $a = 2\lambda$, the attenuation constants for the dominant modes are shown to increase by 20 dB per a by adding a lossless padding layer to a lossy magnetic coating. Application of this result in radar cross section (RCS) reduction is also discussed.**

I. Introduction

THIS PAPER studies multilayered coating on a circular cylindrical waveguide. By lining the interior wall of a waveguide, the modal fields in the waveguide are altered in order to achieve either more or less attenuation for certain modes. In radar cross section (RCS) applications, a high attenuation rate for the dominant modes is desirable whereas in other applications [1]–[7] smaller attenuation rates are desirable.

Our particular application of interest is the reduction of the RCS of a circular waveguide terminated by a perfect electrical conducting (PEC) end plate. Pathak and Altintas [8] showed that the interior irradiation contribution to the RCS of a shorted waveguide is due mainly to a few low-order normal modes. By attenuating low-order modes, a lossy lining layer serves as a mode suppressor, which then reduces the RCS of the cavity. Lee *et al.* [9] studied the normal mode behavior for a circular waveguide lined with a single layer of coating. It was shown that at low frequencies ($a/\lambda \sim 1$, where a = radius of the cylinder; λ = the free-space wavelength) for a slightly lossy coating layer, the low-order modes can be highly attenuated with a single thin layer of coating. As the frequency increases, however, the attenuation constants of most of the low-order modes become small and decrease as a function of λ^2/a^3. Thus, RCS reduction can be achieved only over a fairly narrow frequency range with a single layer of coating. This paper studies the propagation/attenuation constants of the low-order modes in a waveguide lined with multiple layers of coating. By using two or more layers of coating material, the fields inside the waveguide can be more easily manipulated to achieve a greater region of attenuation. With multilayered coating, it is possible to achieve larger attenuation constants over a broader frequency range than with a single layer of coating.

Past studies of coated waveguides have included such methods as perturbation theory [2], [3], [5], transmission-line model [1]–[4], and asymptotic theory [6]. These methods often require simplifying assumptions that are too restrictive, such as that the coating material must be nearly lossless [2]–[4] or very lossy [6]. This treatment will apply the more general method of solving the modal characteristic equation exactly by a numerical method. This is feasible because of the fast computational speed of modern computers and the availability of efficient subroutines for computing Bessel functions with complex arguments.

In Section II an overview of the modal fields in a coated circular waveguide is given. The mathematical formulation for the exact characteristic equation of the normal modes for a circular waveguide with multiple layers of internal coating is presented in Section III. The conventional method involves setting the determinant of a $4n \times 4n$ matrix equal to 0, where n is the number of coating layers.

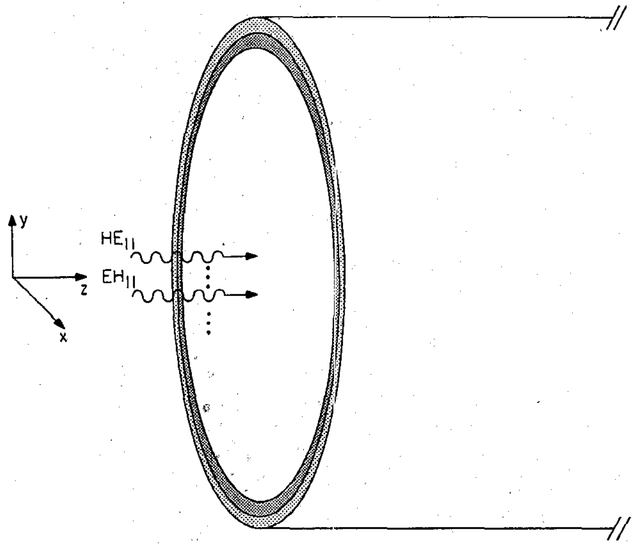

Fig. 1. A coated circular waveguide

Manuscript received September 2, 1987; revised February 16, 1988. This work was supported by NASA under Grant NAG 3-475.

R.-C. Chou was with the Department of Electrical and Computer Engineering, University of Illinois, Urbana. He is now with the ElectroScience Laboratory, Department of Electrical Engineering, The Ohio State University, Columbus, OH 43212.

S.-W. Lee is with the Department of Electrical and Computer Engineering, University of Illinois, Urbana, IL 61801.

IEEE Log Number 8821218.

0018-9480/88/0700-1167$01.00 ©1988 IEEE

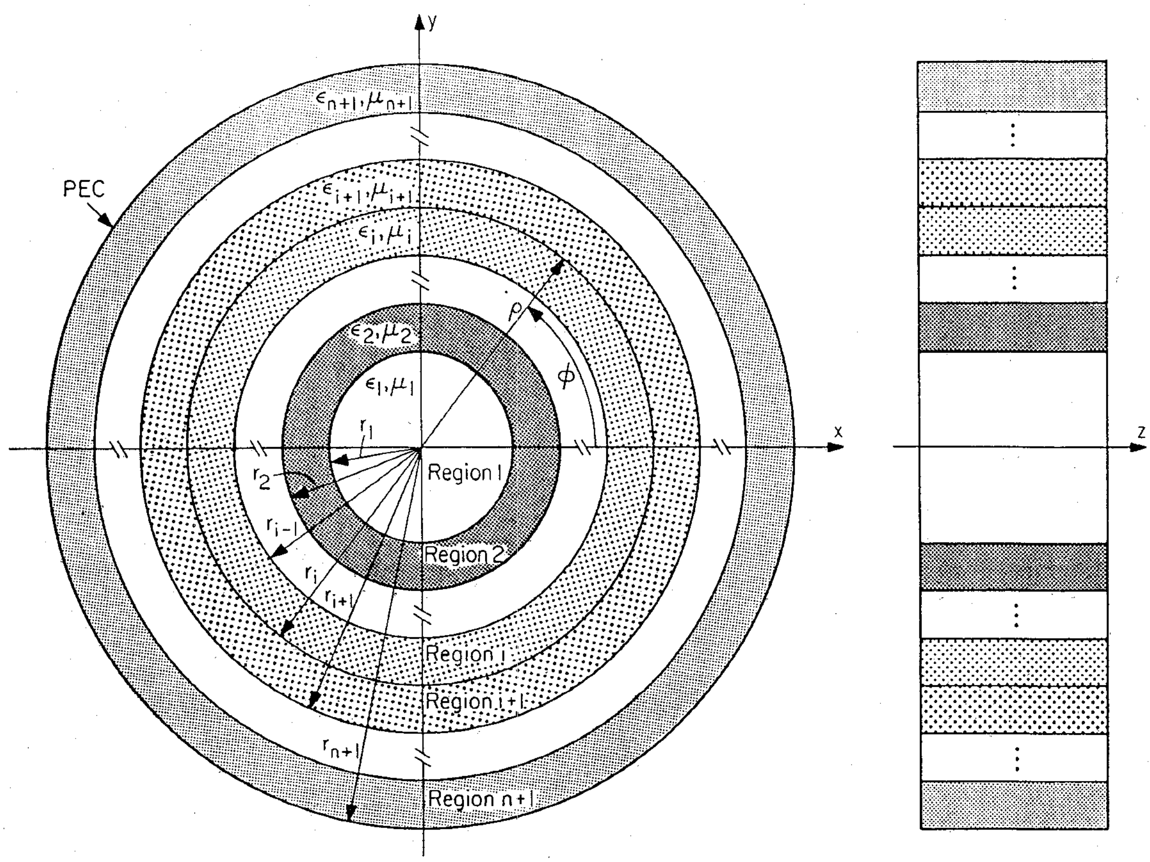

Fig. 2. Exaggerated cross-sectional view of multilayered coated waveguide.

The propagation constants of the normal modes are the solutions of the characteristic equation. As the number of layers increases, this method becomes cumbersome due to the large size of the matrices involved. In addition, the characteristic equation, a transcendental equation involving Bessel functions, must be solved numerically on a computer. Different programs must be written for different numbers of coating layers. A generalized method for formulating the characteristic equation is presented which involves only the manipulation of 4×4 matrices. This method allows for a computer implementation which permits any arbitrary number of coating layers. Numerical results for the attenuation properties of the normal modes of circular waveguides with single and multiple layers of coating are presented in Section IV.

II. Overview of Modal Fields in a Coated Circular Waveguide

A coated cylindrical waveguide is shown in Fig. 1. The problem of interest is the propagation/attenuation properties of the normal modes of such a structure. Fig. 2 shows an exaggerated view of the coating layers for the sake of illustrating the geometrical features of the guide. In the application, the coating layers will be very thin relative to the diameter of the guide. The waveguide walls are assumed to be perfectly conducting, and each coating layer is assumed to be of uniform thickness. The axis of the cylinder coincides with the z axis. Both the permittivity ϵ_i and permeability μ_i of each coating layer are allowed to be complex. The characteristic equation for the propagation constant k_z of the normal modes is derived from the well-known method of seeking nontrivial solutions for the coefficients of the field expressions of the equations obtained by enforcing the continuity of the four tangential fields, H_z, E_z, H_ϕ, E_ϕ, at each interface between two coating layers, and between the innermost coating layer and the inner region [10].

In an uncoated waveguide, the normal modes are either TE_{mn} or TM_{mn} with respect to the longitudinal axis z. The index m describes the azimuthal variation in the form of $\sin m\phi$ or $\cos m\phi$. Here, the index n describes the order of the eigenvalues of $J_m(k_\rho a)=0$ for TM and $J_m'(k_\rho a)=0$ for TE, where J_m is the Bessel function of order m. (Note that variable n is also used to represent the number of coating layers. The intended meaning of subsequent uses of n should be clear from its context.) With the exception of the $m=0$ case, the normal modes are no longer pure TE or TM when the waveguide is coated with dielectric or magnetic material. The modes are commonly classified into HE_{mn} and EH_{mn} in such a way that in the limiting case of a vanishing thin coating [11]

$$HE_{mn} \rightarrow TE_{mn} \quad \text{and} \quad EH_{mn} \rightarrow TM_{mn}. \tag{1}$$

The modal fields for the waveguide are given by

$$E_\rho^1 = \left[-A_1 \frac{k_z k_{\rho 1}}{\omega \epsilon_1} F_1'(\rho) - A_2 \frac{m}{\rho} F_1(\rho) \right] \cos m\phi$$

$$E_\rho^i = \left[-B_1^i \frac{k_z k_{\rho_i}}{\omega \epsilon_i} F_i'(\rho) - B_2^i \frac{k_z k_{\rho_i}}{\omega \epsilon_i} G_i'(\rho) - B_3^i \frac{m}{\rho} F_i(\rho) - B_4^i \frac{m}{\rho} G_i(\rho) \right] \cos m\phi$$

$$E_\rho^{n+1} = \left[-C_1 \frac{k_z k_{\rho_{n+1}}}{\omega \epsilon_{n+1}} K_1'(\rho) - C_2 \frac{m}{\rho} K_2(\rho) \right] \cos m\phi$$

$$E_\phi^1 = \left[-A_1 \frac{k_z m}{\omega \epsilon_1 \rho} F_1(\rho) - A_2 k_{\rho_1} F_1'(\rho) \right] \sin m\phi$$

$$E_\phi^i = \left[-B_1^i \frac{k_z m}{\omega \epsilon_i \rho} F_i(\rho) - B_2^i \frac{k_z m}{\omega \epsilon_i \rho} G_i(\rho) - B_3^i k_{\rho_i} F_i'(\rho) - B_4^i k_{\rho_i} G_i'(\rho) \right] \sin m\phi$$

$$E_\phi^{n+1} = \left[-C_1 \frac{k_z m}{\omega \epsilon_{n+1} \rho} K_1(\rho) - C_2 k_{\rho_{n+1}} K_2'(\rho) \right] \sin m\phi$$

$$E_z^1 = A_1 \frac{k_{\rho_1}^2}{j\omega \epsilon_1} F_1(\rho) \cos m\phi$$

$$E_z^i = \left[B_1^i \frac{k_{\rho_i}^2}{j\omega \epsilon_i} F_i(\rho) + B_2^i \frac{k_{\rho_i}^2}{j\omega \epsilon_i} G_i(\rho) \right] \cos m\phi$$

$$E_z^{n+1} = C_1 \frac{k_{\rho_{n+1}}^2}{j\omega \epsilon_{n+1}} K_1(\rho) \cos m\phi$$

$$H_\rho^1 = \left[-A_1 \frac{m}{\rho} F_1(\rho) - A_2 \frac{k_z k_{\rho_1}}{\omega \mu_1} F_1'(\rho) \right] \sin m\phi$$

$$H_\rho^i = \left[-B_1^i \frac{m}{\rho} F_i(\rho) - B_2^i \frac{m}{\rho} G_i(\rho) - B_3^i \frac{k_z k_{\rho_i}}{\omega \mu_i} F_i'(\rho) - B_4^i \frac{k_z k_{\rho_i}}{\omega \mu_i} G_i'(\rho) \right] \sin m\phi$$

$$H_\rho^{n+1} = \left[-C_1 \frac{k_z m}{\omega \mu_{n+1} \rho} K_1(\rho) - C_2 \frac{k_z k_{\rho_{n+1}}}{\omega \mu_{n+1}} K_2'(\rho) \right] \sin m\phi$$

$$H_\phi^1 = \left[-A_1 k_{\rho_1} F_1'(\rho) - A_2 \frac{k_z m}{\omega \mu_1 \rho} F_1(\rho) \right] \cos m\phi$$

$$H_\phi^i = \left[-B_1^i k_{\rho_i} F_i'(\rho) - B_2^i k_{\rho_i} G_i'(\rho) - B_3^i \frac{k_z m}{\omega \mu_i \rho} F_i(\rho) - B_4^i \frac{k_z m}{\omega \mu_i \rho} G_i(\rho) \right] \cos m\phi$$

$$H_\phi^{n+1} = \left[-C_1 k_{\rho_{n+1}} K_1'(\rho) - C_2 \frac{k_z m}{\omega \mu_{n+1} \rho} K_2(\rho) \right] \cos m\phi$$

$$H_z^1 = A_2 \frac{k_{\rho_1}^2}{j\omega \mu_1} F_1(\rho) \cos m\phi$$

$$H_z^i = \left[B_3^i \frac{k_{\rho_i}^2}{j\omega \mu_i} F_i(\rho) + B_4^i \frac{k_{\rho_i}^2}{j\omega \mu_i} G_i(\rho) \right] \cos m\phi$$

$$H_z^{n+1} = C_1 \frac{k_{\rho_{n+1}}^2}{j\omega \mu_{n+1}} K_2(\rho) \cos m\phi$$

where

$$F_i(\rho) = J_m(k_{\rho_i} \rho)$$
$$F_i'(\rho) = J_m'(k_{\rho_i} \rho)$$
$$G_i(\rho) = N_m(k_{\rho_i} \rho)$$
$$G_i'(\rho) = N_m'(k_{\rho_i} \rho)$$
$$K_1(\rho) = J_m(k_{\rho_{n+1}} \rho) N_m(k_{\rho_{n+1}} r_{n+1}) - N_m(k_{\rho_{n+1}} \rho) J_m(k_{\rho_{n+1}} r_{n+1})$$
$$K_1'(\rho) = J_m'(k_{\rho_{n+1}} \rho) N_m(k_{\rho_{n+1}} r_{n+1}) - N_m'(k_{\rho_{n+1}} \rho) J_m(k_{\rho_{n+1}} r_{n+1})$$
$$K_2(\rho) = J_m(k_{\rho_{n+1}} \rho) N_m'(k_{\rho_{n+1}} r_{n+1}) - N_m(k_{\rho_{n+1}} \rho) J_m'(k_{\rho_{n+1}} r_{n+1})$$
$$K_2'(\rho) = J_m'(k_{\rho_{n+1}} \rho) N_m'(k_{\rho_{n+1}} r_{n+1}) - N_m(k_{\rho_{n+1}} \rho) J_m'(k_{\rho_{n+1}} r_{n+1}). \quad (2)$$

The convention of $\exp[j(\omega t - k_z z)]$ is understood and suppressed. Superscript 1 represents the inner region; superscript $n+1$ represent the layer of coating on the conducting wall; and superscript i represents the ith region, where $2 \leqslant i \leqslant n$. Subscripts ρ, ϕ, and z indicate the radial, angular, and propagation-directional components of the fields, respectively. k_{ρ_i} represents the radial wave vector in region i, where $k_{\rho_i}^2 + k_z^2 = \epsilon_i \mu_i k_0^2$ and $k_0 = 2\pi/\lambda$; ω is the angular frequency; J_m is the Bessel function; and N_m is the Neumann function of order m. A_1, A_2, B_1^i, B_2^i, B_3^i, B_4^i, C_1, and C_2 are the constants, which are determined by the boundary conditions and normalization requirements. Due to circular symmetry, there are two degenerate modes for each angular mode index except for $m = 0$. One of the two degenerate modes is arbitrarily chosen in the above expressions.

III. Characteristic Equation of the Normal Modes

For the case of a single layer of coating, the characteristic equation for the propagation constant k_z of a normal mode is well known [10] and is given by

$$k_{\rho_1}^2\left[F_1'(a)-\epsilon_2\frac{F_1(a)K_1'(a)}{K_1(a)}\frac{k_{\rho_1}}{k_{\rho_2}}\right]\cdot\left[F_1'(a)-\mu_2\frac{F_1(a)K_2'(a)}{K_2(a)}\frac{k_{\rho_1}}{k_{\rho_2}}\right]-\left[\frac{k_z m}{(k_0 a)}\right]F_1^2(a)\left[1-\left(\frac{k_{\rho_1}}{k_{\rho_2}}\right)^2\right]^2=0 \qquad (3)$$

where

$$a=r_1$$

$$b=r_2$$

$$k_{\rho_1}^2+k_z^2=k_0^2$$

$$k_{\rho_2}^2+k_z^2=\epsilon_2\mu_2k_0^2.$$

For a double layer of coating, the characteristic equation for the propagation constant k_z of the modal fields is given by the 8×8 matrix equation

$$\det\begin{vmatrix}
\frac{k_{\rho_1}^2}{\epsilon_1}F_1(a) & 0 & \frac{-k_{\rho_2}^2}{\epsilon_2}F_2(a) & \frac{-k_{\rho_2}^2}{\epsilon_2}G_2(a) & 0 & 0 & 0 & 0\\
0 & 0 & \frac{k_{\rho_2}^2}{\epsilon_2}F_2(b) & \frac{k_{\rho_2}^2}{\epsilon_2}G_2(b) & 0 & 0 & \frac{-k_{\rho_3}^2}{\epsilon_3}\mathrm{K}_1(b) & 0\\
0 & \frac{k_{\rho_1}^2}{\mu_1}F_1(a) & 0 & 0 & \frac{-k_{\rho_2}^2}{\mu_2}F_2(a) & \frac{-k_{\rho_2}^2}{\mu_2}G_2(a) & 0 & 0\\
0 & 0 & 0 & 0 & \frac{k_{\rho_2}^2}{\mu_2}F_2(b) & \frac{k_{\rho_2}^2}{\mu_2}G_2(b) & 0 & \frac{-k_{\rho_3}^2}{\mu_3}\mathrm{K}_2(b)\\
k_{\rho_1}F_1'(a) & \frac{k_zm}{\omega a}\frac{1}{\mu_1}F_1(a) & -k_{\rho_2}F_2'(a) & -k_{\rho_2}G_2'(a) & \frac{-k_zm}{\omega a}\frac{1}{\mu_2}F_2(a) & \frac{-k_zm}{\omega a}\frac{1}{\mu_2}G_2(a) & 0 & 0\\
0 & 0 & k_{\rho_2}F_2'(b) & k_{\rho_2}G_2'(b) & \frac{k_zm}{\omega b}\frac{1}{\mu_2}F_2(b) & \frac{k_zm}{\omega b}\frac{1}{\mu_2}G_2(b) & -k_{\rho_3}\mathrm{K}_1'(b) & \frac{-k_zm}{\omega b}\frac{1}{\mu_3}\mathrm{K}_2(b)\\
\frac{k_zm}{\omega a}\frac{1}{\epsilon_1}F_1(a) & k_{\rho_1}F_1'(a) & \frac{-k_zm}{\omega a}\frac{1}{\epsilon_2}F_2(a) & \frac{-k_zm}{\omega a}\frac{1}{\epsilon_2}G_2(a) & -k_{\rho_2}F_2'(a) & -k_{\rho_2}G_2'(a) & 0 & 0\\
0 & 0 & \frac{k_zm}{\omega b}\frac{1}{\epsilon_2}F_2(b) & \frac{k_zm}{\omega b}\frac{1}{\epsilon_2}G_2(b) & k_{\rho_2}F_2'(b) & k_{\rho_2}G_2(b) & \frac{-k_zm}{\omega b}\frac{1}{\epsilon_3}\mathrm{K}_1(b) & -k_{\rho_3}\mathrm{K}_2'(b)
\end{vmatrix}=0 \qquad (4)$$

where $a=r_1$, $b=r_2$, and $c=r_3$.

In general, for n layers of coating, the characteristic equation for k_z is given by a $4n\times4n$ matrix equation. In numerically solving the equation, the computer time required becomes cumbersome as the number of layers increases. An efficient method for formulating the characteristic equation [12] for an arbitrary number of layers can be utilized which involves only the manipulation of 4×4 matrices.

The boundary matching equations at each media interface can be written as 4×4 matrix equations, At $\rho=r_1$ (boundary between region 1, center region, and region 2, innermost layer),

$$\begin{bmatrix}
\frac{k_{\rho_1}^2}{\epsilon_1}F_1(r_1) & 0 & 0\\
0 & \frac{k_{\rho_1}^2}{\mu_1}F_1(r_1) & 0\\
k_{\rho_1}F_1'(r_1) & \frac{k_zm}{\omega r_1}\frac{1}{\mu_1}F_1(r_1) & 0\\
\frac{k_zm}{\omega r_1}\frac{1}{\epsilon_1}F_1(r_1) & k_{\rho_1}F_1'(r_1) & 0
\end{bmatrix}\begin{bmatrix}A_1\\A_2\\0\\0\end{bmatrix}=\begin{bmatrix}
\frac{k_{\rho_2}^2}{\epsilon_2}F_2(r_1) & \frac{k_{\rho_2}^2}{\epsilon_2}G_2(r_1) & 0 & 0\\
0 & 0 & \frac{k_{\rho_2}^2}{\mu_2}F_2(r_1) & \frac{k_{\rho_2}^2}{\mu_2}G_2(r_1)\\
k_{\rho_2}F_2'(r_1) & k_{\rho_2}G_2'(r_1) & \frac{k_zm}{\omega r_1}\frac{1}{\mu_2}F_2(r_1) & \frac{k_zm}{\omega r_1}\frac{1}{\mu_2}G_2(r_1)\\
\frac{k_zm}{\omega r_1}\frac{1}{\epsilon_2}F_2(r_1) & \frac{k_zm}{\omega r_1}\frac{1}{\epsilon_2}G_2(r_1) & k_{\rho_2}F_2'(r_1) & k_{\rho_2}G_2'(r_1)
\end{bmatrix}\begin{bmatrix}B_1^2\\B_2^2\\B_3^2\\B_4^2\end{bmatrix}. \qquad (5)$$

At $\rho = r_i$, $2 \leqslant i \leqslant n-1$ (boundary between region i and $i+1$),

$$
\begin{bmatrix}
\frac{k_{\rho_i}^2}{\epsilon_i}F_i(r_i) & \frac{k_{\rho_i}^2}{\epsilon_i}G_i(r_i) & 0 & 0 \\
0 & 0 & \frac{k_{\rho_i}^2}{\mu_i}F_i(r_i) & \frac{k_{\rho_i}^2}{\mu_i}G_i(r_i) \\
k_{\rho_i}F_i'(r_i) & k_{\rho_i}G_i'(r_i) & \frac{k_z m}{\omega r_i}\frac{1}{\mu_i}F_i(r_i) & \frac{k_z m}{\omega r_i}\frac{1}{\mu_i}G_i(r_i) \\
\frac{k_z m}{\omega r_i}\frac{1}{\epsilon_i}F_i(r_i) & \frac{k_z m}{\omega r_i}\frac{1}{\epsilon_i}G_i(r_i) & k_{\rho_i}F_i'(r_i) & k_{\rho_i}G_i'(r_i)
\end{bmatrix}
\begin{bmatrix} B_1^i \\ B_2^i \\ B_3^i \\ B_4^i \end{bmatrix}
$$

$$
= \begin{bmatrix}
\frac{k_{\rho_i}^2}{\epsilon_{i+1}}F_{i+1}(r_i) & \frac{k_{\rho_1}^2}{\epsilon_{i+1}}G_{i+1}(r_i) & 0 & 0 \\
0 & 0 & \frac{k_{\rho_i}^2}{\mu_{i+1}}F_{i+1}(r_i) & \frac{k_{\rho_i}^2}{\mu_{i+1}}G_{i+1}(r_i) \\
k_{\rho_i}F_{i+1}'(r_i) & k_{\rho_i}G_{i+1}'(r_i) & \frac{k_z m}{\omega r_i}\frac{1}{\mu_{i+1}}F_{i+1}(r_i) & \frac{k_z m}{\omega r_i}\frac{1}{\mu_{i+1}}G_{i+1}(r_i) \\
\frac{k_z m}{\omega r_i}\frac{1}{\epsilon_{i+1}}F_{i+1}(r_i) & \frac{k_z m}{\omega r_i}\frac{1}{\epsilon_{i+1}}G_{i+1}(r_i) & k_{\rho_i}F_{i+1}'(r_i) & k_{\rho_i}G_{i+1}'(r_i)
\end{bmatrix}
\begin{bmatrix} B_1^{i+1} \\ B_2^{i+1} \\ B_3^{i+1} \\ B_4^{i+1} \end{bmatrix}. \tag{6}
$$

At $\rho = r_n$ (boundary between two most outermost layers),

$$
\begin{bmatrix}
\frac{k_{\rho_n}^2}{\epsilon_n}F_n(r_n) & \frac{k_{\rho_n}^2}{\epsilon_n}G_n(r_n) & 0 & 0 \\
0 & 0 & \frac{k_{\rho_n}^2}{\mu_n}F_n(r_n) & \frac{k_{\rho_n}^2}{\mu_n}G_n(r_n) \\
k_{\rho_n}F_n'(r_n) & k_{\rho_n}G_n'(r_n) & \frac{k_z m}{\omega r_n}\frac{1}{\mu_n}F_n(r_n) & \frac{k_z m}{\omega r_n}\frac{1}{\mu_n}G_n(r_n) \\
\frac{k_z m}{\omega r_n}\frac{1}{\epsilon_n}F_n(r_n) & \frac{k_z m}{\omega r_n}\frac{1}{\epsilon_n}G_n(r_n) & k_{\rho_1}F_n'(r_n) & k_{\rho_1}G_n'(r_n)
\end{bmatrix}
\begin{bmatrix} B_1^n \\ B_2^n \\ B_3^n \\ B_4^n \end{bmatrix}
=
\begin{bmatrix}
\frac{k_{\rho_{n+1}}^2}{\epsilon_{n+1}}K_1(r_n) & 0 & 0 & 0 \\
0 & \frac{k_{\rho_{n+1}}^2}{\mu_{n+1}}K_2(r_n) & 0 & 0 \\
k_{\rho_{n+1}}K_1'(r_n) & \frac{k_z m}{\omega r_n}\frac{1}{\mu_{n+1}}K_2(r_n) & 0 & 0 \\
\frac{k_z m}{\omega r_n}\frac{1}{\epsilon_{n+1}}K_1(r_n) & k_{\rho_{n+1}}K_2'(r_n) & 0 & 0
\end{bmatrix}
\begin{bmatrix} C_1 \\ C_2 \\ 0 \\ 0 \end{bmatrix}. \tag{7}
$$

The boundary matching equations thus become n matrix equations for n layers of coating:

$$
\begin{aligned}
\boldsymbol{M}_{11}\boldsymbol{A} &= \boldsymbol{M}_{21}\boldsymbol{B} \\
\boldsymbol{M}_{22}\boldsymbol{B} &= \boldsymbol{M}_{32}\boldsymbol{B} \\
&\vdots \\
\boldsymbol{M}_{nn}\boldsymbol{B} &= \boldsymbol{M}_{(n+1)n}\boldsymbol{C}.
\end{aligned} \tag{8}
$$

$\boldsymbol{M}_{ab}$ refers to the matrix resulting from the tangential fields in region a matched at boundary r_b. $\boldsymbol{A}$ is then related to $\boldsymbol{C}$ by

$$\boldsymbol{M}_{11}\boldsymbol{A} = \boldsymbol{M}_{21}\boldsymbol{M}_{22}^{-1} \cdots \boldsymbol{M}_{nn}^{-1}\boldsymbol{M}_{(n+1)n}\boldsymbol{C} \tag{9}$$

or

$$\boldsymbol{M}_{11}\boldsymbol{A} = \boldsymbol{M}\boldsymbol{C}$$

where

$$\boldsymbol{M} = \boldsymbol{M}_{21}\boldsymbol{M}_{22}^{-1} \cdots \boldsymbol{M}_{nn}^{-1}\boldsymbol{M}_{(n+1)n}.$$

Because the last two columns of $\boldsymbol{M}_{(n+1)n}$ are zero vectors, the last two columns of $\boldsymbol{M}$ will also be zero vectors. Therefore, $\boldsymbol{M}$ will be in form

$$
\boldsymbol{M} = \begin{bmatrix}
m_{11} & m_{12} & 0 & 0 \\
m_{21} & m_{22} & 0 & 0 \\
m_{31} & m_{32} & 0 & 0 \\
m_{41} & m_{42} & 0 & 0
\end{bmatrix}. \tag{10}
$$

Equation (9) written out is then

$$\begin{bmatrix} \frac{k_{\rho_1}^2}{\epsilon_1}F_1(r_1) & 0 & 0 & 0 \\ 0 & \frac{k_{\rho_1}^2}{\mu_1}F_1(r_1) & 0 & 0 \\ k_{\rho_1}F'(r_1) & \frac{k_z m}{\omega r_1}\frac{1}{\epsilon_1}F_1(r_1) & 0 & 0 \\ \frac{k_z m}{\omega r_1}\frac{1}{\epsilon_1}F_1(r_1) & k_{\rho_1}F_1'(r_1) & 0 & 0 \end{bmatrix}\begin{bmatrix} A_1 \\ A_2 \\ 0 \\ 0 \end{bmatrix} = \begin{bmatrix} m_{11} & m_{12} & 0 & 0 \\ m_{21} & m_{22} & 0 & 0 \\ m_{31} & m_{32} & 0 & 0 \\ m_{41} & m_{42} & 0 & 0 \end{bmatrix}\begin{bmatrix} C_1 \\ C_2 \\ 0 \\ 0 \end{bmatrix} \tag{11}$$

which can be rewritten as

$$\begin{bmatrix} \frac{k_{\rho_1}^2}{\epsilon_1}F_1(r_1) & 0 & -m_{11} & -m_{12} \\ 0 & \frac{k_{\rho_1}^2}{\mu_1}F_1(r_1) & -m_{21} & -m_{22} \\ k_{\rho_1}F'(r_1) & \frac{k_z m}{\omega r_1}\frac{1}{\epsilon_1}F_1(r_1) & -m_{31} & -m_{32} \\ \frac{k_z m}{\omega r_1}\frac{1}{\epsilon_1}F_1(r_1) & k_{\rho_1}F_1'(r_1) & -m_{41} & -m_{42} \end{bmatrix}\cdot\begin{bmatrix} A_1 \\ A_2 \\ C_1 \\ C_2 \end{bmatrix} = 0. \tag{12}$$

A_1, A_2, and C_1, C_2 fully define the fields in the inner region and outermost layer, respectively. The characteristic equation for the propagation constant k_z is then given by the determinant of the 4×4 matrix $\boldsymbol{M}_{AC}$ set equal to zero, where $\boldsymbol{M}_{AC}$ is the 4×4 matrix in (12):

$$\det \boldsymbol{M}_{AC} = \det\begin{bmatrix} \frac{k_{\rho_1}^2}{\epsilon_1}F_1(r_1) & 0 & -m_{11} & -m_{12} \\ 0 & \frac{k_{\rho_1}^2}{\mu_1}F_1(r_1) & -m_{21} & -m_{22} \\ k_{\rho_1}F'(r_1) & \frac{k_z m}{\omega r_1}\frac{1}{\epsilon_1}F_1(r_1) & -m_{31} & -m_{32} \\ \frac{k_z m}{\omega r_1}\frac{1}{\epsilon_1}F_1(r_1) & k_{\rho_1}F_1'(r_1) & -m_{41} & -m_{42} \end{bmatrix} = 0. \tag{13}$$

To summarize, the boundary field matching equations can be expressed in the form of the 4×4 matrix equations (5), (6), and (7). From these relations, the coefficients for the fields in the center uncoated region can be shown to be related to the coefficients in the outermost coating layer by (9), which can be expressed as (12). Finally, for nontrivial solutions of the modal fields, the 4×4 matrix in (12) must be singular. Thus, the characteristic equation for the propagation constants of the normal modes is given by (13).

All manipulations now involve only the inversion and multiplication of 4×4 matrices. Using this formulation, a computer program to compute the propagation constant k_z for any arbitrary number of coating layers can be written. The final expression (13), a complex transcendental equation, can be solved numerically using, for example, Müller's method (available as an International Mathematical Statistical Libraries subroutine.)

IV. Numerical Results

The attenuation constant α of a normal mode in a coated waveguide is related to the magnetic and electric energies in the coated regions, $|H|^2$ and $|E|^2$, by

$$\alpha \propto \int_v \left[\operatorname{Im}|\mu|^2|H|^2 + \operatorname{Im}|\epsilon|^2|E|^2\right] dV \tag{14}$$

where the volume of integration is over the coated region [10]. Because of the boundary condition of the PEC waveguide wall, the magnetic energy of an empty waveguide is much larger than the electric energy near the surface. Since the fields of the waveguide are not perturbed significantly by a coating layer in the low-frequency region, a lossy and magnetic coating material is effective in reducing the RCS of a coated waveguide. Lee *et al.* [13] theoretically predicted and experimentally verified a 20 dBSM reduction for a PEC-terminated waveguide ($a/\lambda = 0.98$) lined with a lossy magnetic coating material with a thickness of only 1.18 percent of the radius. As such, the numerical results pre-

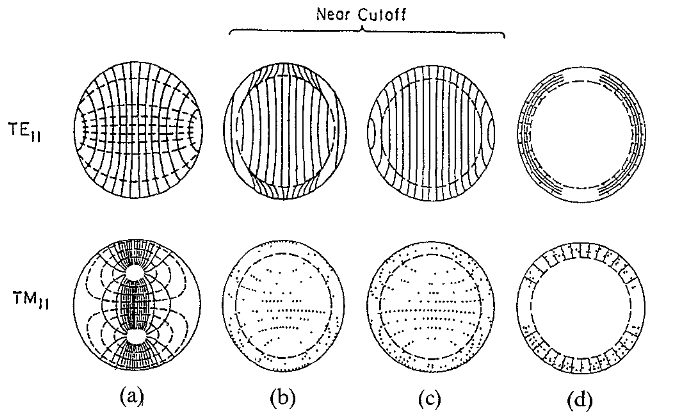

Fig. 3. Transverse field distributions of the normal modes in (a) empty waveguide, (b) dielectric coated waveguide ($\epsilon_r = 10.0$, $\mu_r = 1.0$) at cutoff frequencies, (c) magnetic coated waveguide ($\epsilon_r = 1.0$, $\mu_r = 10.0$) at cutoff frequencies, and (d) coated waveguide at the high-frequency limit.

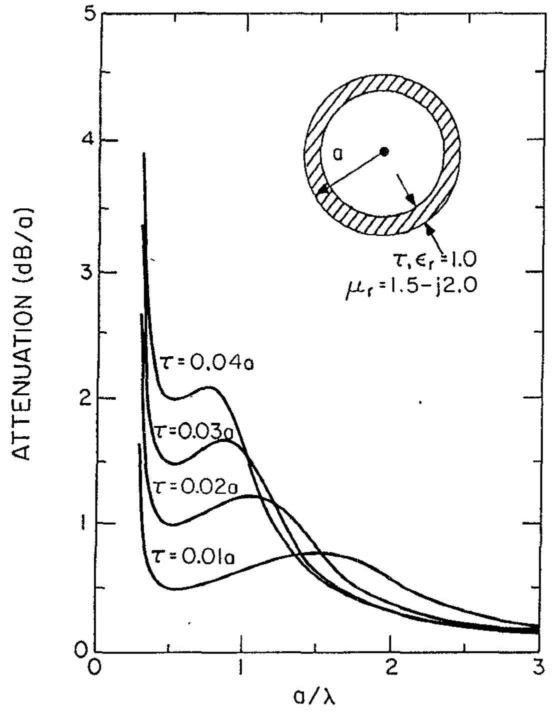

Fig. 4. Attenuation constants of the HE_{11} mode in a lossy magnetic coated waveguide ($\epsilon_r = 1.0$, $\mu_r = 1.5 - j2.0$).

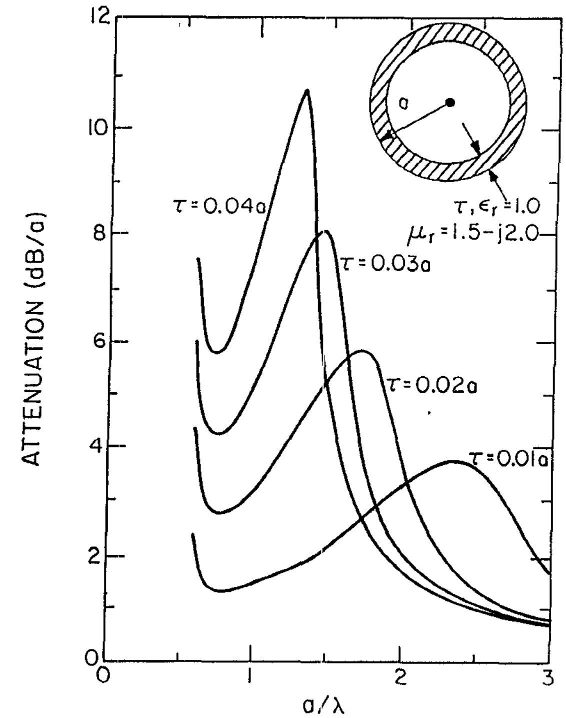

Fig. 5. Attenuation constants of the EH_{11} mode in a lossy magnetic coated waveguide ($\epsilon_r = 1.0$, $\mu_r = 1.5 - j2.0$).

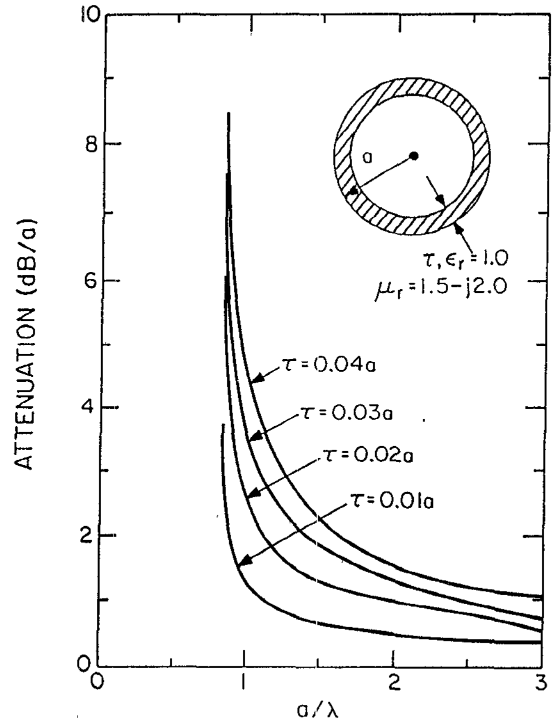

Fig. 6. Attenuation constants of the HE_{12} mode in a lossy magnetic coated waveguide ($\epsilon_r = 1.0$, $\mu_r = 1.5 - j2.0$).

sented will focus on coating configurations involving magnetic layers.

The attenuation properties of the two dominant low-order modes for near-axial-incidence RCS, the HE_{11} and EH_{11} modes, will be discussed for single- and double-layer coating schemes. The interior uncoated region is taken to be free space ($\epsilon = \epsilon_0$, $\mu = \mu_0$) in all cases. The transverse field distributions for the two modes are shown in Fig. 3 for (a) empty guide, (b) lossless dielectric coated guide near cutoff, (c) lossless magnetic coated guide near cutoff, and (d) lossless coated guide in the high frequency limit.

A. Review of Single-Layer Coating Results

With a layer of lossy coating material, the low-order modes of a circular waveguide become inner modes [9] as a/λ increases. The field distribution for such modes is confined mostly in the center region. The fields decay very rapidly from the coating interface to the lossy layer, and the attenuation constants are small. Figs. 4–6 show the attenuation constants as a function of increasing frequency for the HE_{11} and EH_{11} modes, as well as for the HE_{12} mode, in a lossy magnetic ($\mu_r = 1.5 - j2.0$) coated wave-

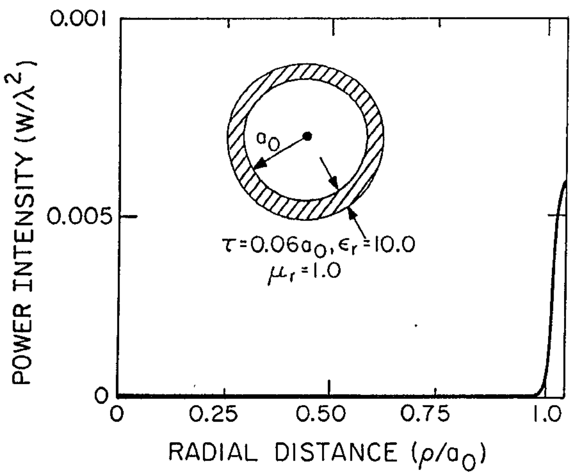

Fig. 7. Normalized angle-averaged power distribution in W/λ^2 as a function of radial distance in a dielectric coated guide ($\epsilon_r = 10.0$, $\mu_r = 1.0$).

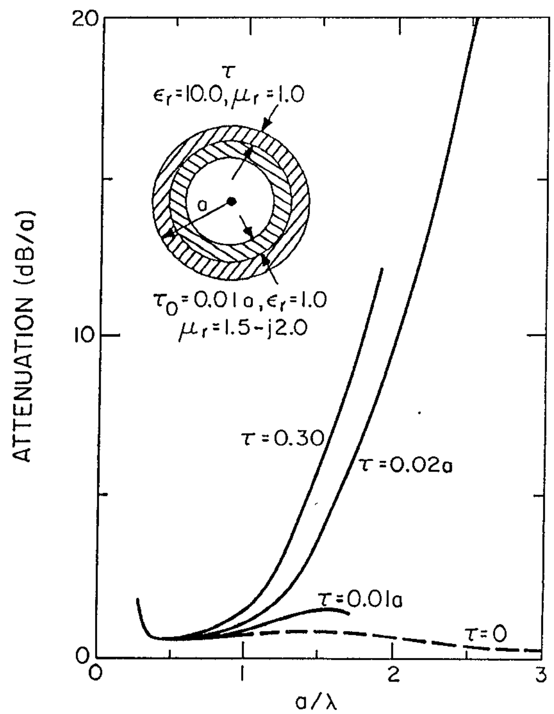

Fig. 8. Attenuation constants of the HE_{11} mode in a double-layer coated waveguide with an inner layer of lossy magnetic material ($\epsilon_r = 1.0$, $\mu_r = 1.5 - j2.0$) and an outer layer of lossless dielectric material ($\epsilon_r = 10.0$, $\mu_r = 1.0$). The thickness of the inner layer is fixed while that for the outer layer is varied.

guide. As the frequency increase, the lossy material tends to expel the fields from the coating region. The attenuation constants decrease as a function of λ^2/a^3 for large frequencies [9].

If the coating material is lossless, however, the modal power distribution is largely concentrated in the coating region. A layer of high dielectric constant tends to "pull" the fields into the coating region as the frequency increases. As shown in Fig. 7, although the dielectric layer ($\epsilon_r = 10.0$) covers only 12 percent of the waveguide cross section, 99 percent of the power is confined in the dielec-

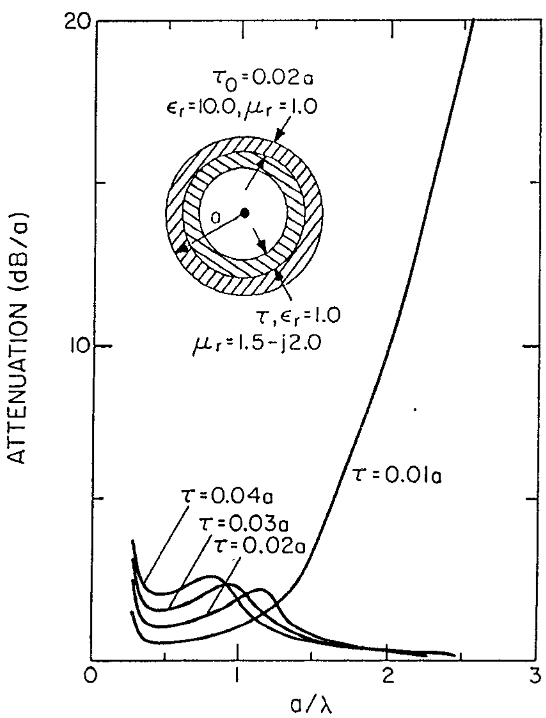

Fig. 9. Attenuation constants of the HE_{11} mode in a double-layer coated waveguide with an inner layer of lossy magnetic material ($\epsilon_r = 1.0$, $\mu_r = 1.5 - j2.0$) and an outer layer of lossless dielectric material ($\epsilon_r = 10.0$, $\mu_r = 1.0$). The thickness of the outer layer is fixed while that for the inner layer is varied.

tric layer. These results suggest that by using a double layer of coating consisting of a lossy layer and a lossless layer with a large permittivity, the high attenuation region of some of the modes of the waveguide can be extended. A high field concentration would be attracted by the lossless dielectric layer into the coating region, and attenuated by the lossy layer. In the following multilayered coating results, the lossless dielectric layer will have $\epsilon_r = 10.0$, and the lossy magnetic layer will have $\mu_r = 1.5 - j2.0$.

B. Multilayered Coating

Figs. 8 and 9 show the TE_{11} attenuation constant as a function of increasing frequency for a lossless dielectric layer sandwiched between the waveguide wall and a lossy magnetic layer. Fig. 8 shows a family of curves for a fixed thickness of lossy material and varying thicknesses of lossy dielectric material. As the dielectric layer increases in thickness, a greater amount of the field energy will be concentrated in this layer. This also causes more of the field to be within the lossy layer, resulting in greater attenuation. Note that there is a significant increase in both the level of attenuation and the frequency band of high attenuation. In Fig. 9, the thickness of the lossy layer is varied while the thickness of the lossless layer is increased. If the lossy layer becomes too thick, the field repulsion property of the lossless layer is dominant over the field attraction property of the lossless layer. Fig. 10 reverses the lossless and the lossy layers so that the lossless layer is towards the waveguide center. No significant in-

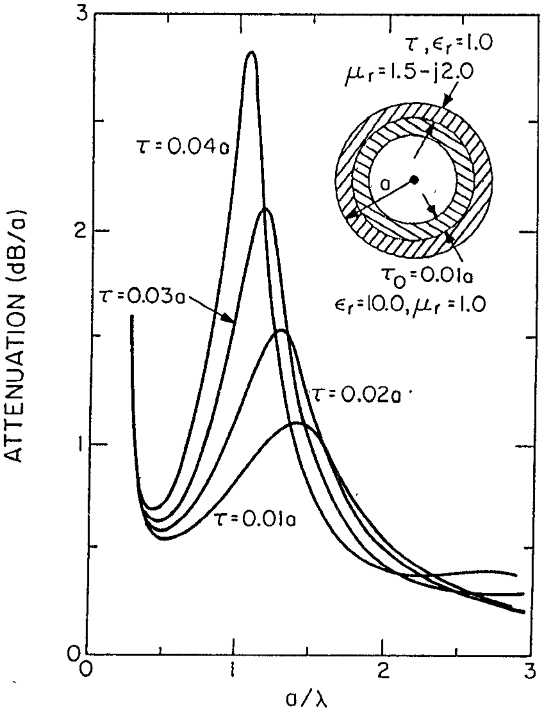

Fig. 10. Attenuation constants of the HE_{11} mode in a double-layer coated waveguide with an inner layer of lossless dielectric material ($\epsilon_r = 10.0$, $\mu_r = 1.0$) and an outer layer of lossy magnetic material ($\epsilon_r = 1.0$, $\mu_r = 1.5 - j2.0$). The thickness of the inner layer is fixed while that for the outer layer is varied.

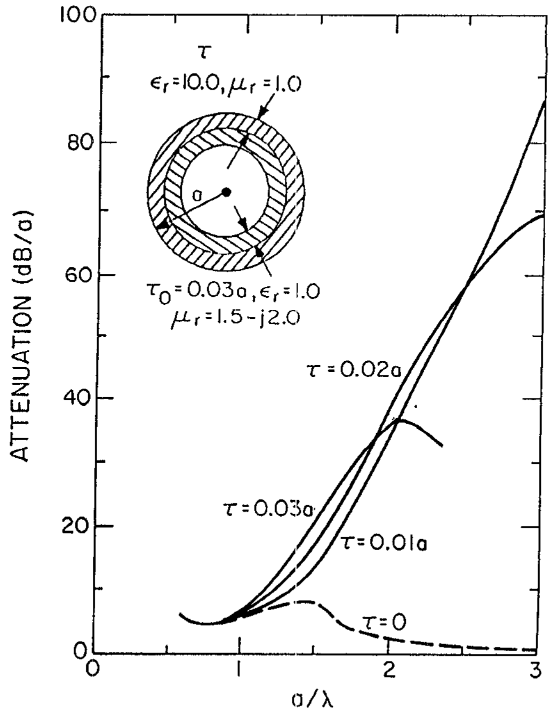

Fig. 11. Attenuation constants of the EH_{11} mode in a double-layer coated waveguide with an inner layer of lossy magnetic material ($\epsilon_r = 1.0$, $\mu_r = 1.5 - j2.0$) and an outer layer of lossless dielectric material ($\epsilon_r = 10.0$, $\mu_r = 1.0$). The thickness of the inner layer is fixed while that for the outer layer is varied.

crease in attenuation is achieved with this configuration for the TE_{11} mode.

Finally, Fig. 11 shows the EH_{11} attenuation constant as a function of increasing frequency for the waveguide wall–lossless layer–lossy layer geometry. The family of curves represents a fixed thickness of the lossy layer and varying thicknesses of the lossless layer. Again, there is a significantly higher level of modal attenuation over a wider frequency band for the multilayered case compared to that of a single layer of the lossy coating case. Note that the maximum value of the attenuation axis is now 100 dB/a (a = radius of cylinder). It is interesting to observe that up to $a/\lambda \sim 2.0$, a thicker lossless layer results in a higher attenuation. But for $a/\lambda > 2.0$, the $\tau = 0.01a$ case results in the highest attenuation. This geometry, though, is not an effective coating for the HE_{11} mode (Fig. 8).

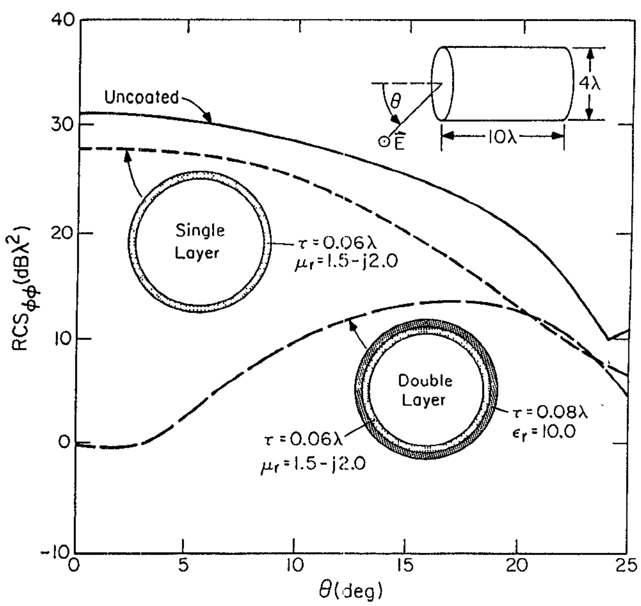

Fig. 12. RCS's of coated and uncoated circular cylinders with diameter 4λ and depth 10λ.

C. Radar Cross Section Reduction

The application of interest is the reduction of RCS of coated cavity structures. In such applications, the actual coating geometry must be optimized to effectively attenuate all the highly excited modes. Detailed discussion of the evaluation of the RCS from a coated waveguide can be found in [14]. Fig. 12 shows the theoretical RCS calculations for a length of circular waveguide terminated with a flat PEC plate. The diameter of the guide is 4λ, and the length is 10λ. The three curves correspond to the RCS of (i) an empty guide, (ii) a waveguide coated with a single layer of lossy magnetic coating, and (iii) a multilayered coated waveguide consisting of a lossless dielectric layer sandwiched between the waveguide wall and a lossy layer. For the given size of the structure, the single layer coating is not very effective in reducing the RCS. However, a double layer coating results in a substantial reduction in the RCS of the cavity at near-axial incidence. When the angel of incidence of the incoming plane wave $\theta \cong 20°$, the three curves approach a similar level. This is due to the fact that the higher order modes are now more strongly excited, and the chosen coating geometry is not effective in attenuating these modes.

V. Conclusions

This paper studied modal attenuation in coated waveguide structures. An overview of the modal fields in a coated circular waveguide was given. To avoid dealing with excessively large matrices, a method was shown to express the waveguide characteristic equation for any number of coating layers which involves only the manipulation of 4×4 matrices. This method was applied to study modal attenuation in a multilayered coated waveguide.

The dominant contributors to the RCS of a PEC-terminated waveguide at near-axial incidence are the low-order modes. A thin single layer of lossy magnetic material can greatly attenuate these modes, and thus reduce the RCS of a waveguide cavity. However, this is only effective over a narrow frequency band at low frequencies. With the proper combination of lossless dielectric coating and lossy magnetic coating, it was shown that a significantly higher modal attenuation can be attained over a broader frequency band for the HE_{11} and EH_{11} modes. For large off-axis incidence, higher order modes come into importance. It should be possible to reduce these modes over a broad frequency band with the proper combination of three or more layers of coating.

Acknowledgment

Discussions with Dr. C. S. Lee in the preparation of this work are gratefully acknowledged.

References

[1] M. Miyagi, A. Hongo, and S. Kawakami, "Transmission characteristics of dielectric-coated metallic waveguide for infrared transmission: Slab waveguide model," *IEEE J. Quantum Electron.*, vol. QE-19, pp. 136–145, Feb. 1983.

[2] H. G. Unger, "Lined waveguide," *Bell Sys. Tech. J.*, vol. 41, pp. 745–768, Mar. 1962.

[3] J. W. Carlin and P. D'Agostino, "Low-loss modes in dielectric lined waveguide," *Bell Sys. Tech. J.*, vol. 50, pp. 1631–1638, May–June 1971.

[4] J. W. Carlin and P. D'Agostino, "Normal modes in overmoded dielectric-lined circular waveguide," *Bell Sys. Tech. J.*, vol. 52, pp. 453–486, Apr. 1973.

[5] E. A. J. Marcatili and R. A. Schmeltzer, "Hollow metallic and dielectric waveguides for long distance optical transmission and lasers," *Bell Sys. Tech. J.*, vol. 43, pp. 1783–1809, July 1964.

[6] C. Dragone, "High-frequency behavior of waveguides with finite surface impedances," *Bell Sys. Tech. J.*, vol. 60, pp. 89–116, Jan. 1981.

[7] M. Miyagi and S. Kawakami, "Design theory of dielectric-coated metallic waveguides for infrared transmission," *J. Lightwave Technol.*, vol. LT-2, no. 2, pp. 114–126, Apr. 1984.

[8] P. H. Pathak and A. Altintas, "An efficient approach for analyzing the EM coupling into large open-ended waveguide cavities," in *1985 North American Radio Science Meeting Dig.* (Vancouver, Canada), 1985, p. 216.

[9] C. S. Lee, S. W. Lee, and S. L. Chuang, "Normal modes in an overmoded circular waveguide coated with lossy material," *IEEE Trans. Microwave Theory Tech.*, vol. MTT-34, pp. 773–785, July 1986.

[10] R. F. Harrington, *Time Harmonic Electromagnetic Fields*. New York: McGraw-Hill, 1961.

[11] P. J. B. Clarricoats, "Propagation along unbounded and bounded dielectric rods," Part 1 and Part 2, *Proc. Inst. Elec. Eng.*, Mon. 409E and 410E, pp. 170–186, Oct. 1960.

[12] C. Yeh and G. Lindgren, "Computing the propagation characteristics of radially stratified fibers: An efficient method," *Appl. Opt.*, vol. 16, pp. 483–493, Feb. 1977.

[13] C. S. Lee, S. W. Lee, and R. Chou, "RCS reduction of a cylindrical cavity by dielectric coating," in *Int. IEEE/AP-S Symp. Dig.* (Philadelphia), June 1986, pp. 305–308.

[14] C. S. Lee and S. W. Lee, "RCS of a coated circular waveguide terminated by a perfect conductor," *IEEE Trans. Atennas Propagat.*, vol. AP-35, pp. 391–398, Apr. 1987.

Ri-Chee Chou (S'84–M'88) was born in Taipei, Taiwan, on October 11, 1961. He received the B.S. degree (with honors) from the California Institute of Technology, Pasadena, in 1983, the M.S. degree from Stanford University, Palo Alto, CA, in 1985, and the Ph.D. degree from the University of Illinois at Urbana-Champaign in 1987, all in electrical engineering.

He is currently an assistant professor of electrical engineering with the ElectroScience Laboratory at The Ohio State University. From 1985 to 1987, he was a research assistant with the Electromagnetic Laboratory at the University of Illinois. Previous to that, he was with the Antenna Department at Lockheed Missiles and Space, Sunnyvale, CA, working on such projects as reflector antenna, frequency selective surfaces, and ultra-broad-band feed arrays. In 1983 he was with Aerojet Electrosystems, Azusa, CA, working on the design and testing of microstrip phased array antennas. His current research interests include realistic modeling in electromagnetic scattering and high-frequency ray techniques.

Shung-Wu Lee (S'83–M'66–SM'73–F'81) was born in Kiangsi, China. He received the B.S. degree in electrical engineering from Cheng Kung University in Tainan, Taiwan, in 1961, and the M.S. and Ph.D. degrees in electrical engineering from the University of Illinois at Urbana.

Currently, he is a professor of electrical and computer engineering and an Associate Director of the Electromagnetics Laboratory at the University of Illinois. He has been on the University's faculty since 1966. While on leave from the University of Illinois, Dr. Lee was with the Hughes Aircraft Company, Fullerton CA, (1969–1970), the Technical University at Eindhoven, The Netherlands, and the University of London, England (1973–1974).

Dr. Lee has published more than 100 papers in technical journals on antennas and electromagnetic theory. He is the coauthor of a book on guided waves published by Macmillan in 1971, and a coauthor of an antenna handbook published in 1986 by Howard W. Sams and Co. He has received several professional awards, including the 1968 Everitt Teaching Excellence Award from the University of Illinois, a 1973 NSF NATO Senior Scientist Fellowship, a 1977 Best Paper Award from IEEE Antennas and Propagation Society, and the 1985 Lockheed Million Dollar Award.